PHYSICAL REVIEW E **83**, 035301(R) (2011)

Random walk of a swimmer in a low-Reynolds-number medium

Michaël Garcia, Stefano Berti, Philippe Peyla, and Salima Rafaï
Université de Grenoble 1/CNRS, LIPhy UMR 5588, Grenoble F-38041, France
(Received 29 November 2010; revised manuscript received 4 February 2011; published 18 March 2011)

Swimming at a micrometer scale demands particular strategies. When inertia is negligible compared to viscous forces, hydrodynamics equations are reversible in time. To achieve propulsion, microswimmers must therefore deform in a way that is not invariant under time reversal. Here, we investigate dispersal properties of the microalga *Chlamydomonas reinhardtii* by means of microscopy and cell tracking. We show that tracked trajectories are well modeled by a correlated random walk. This process is based on short time correlations in the direction of movement called persistence. At longer times, correlation is lost and a standard random walk characterizes the trajectories. Moreover, high-speed imaging enables us to show how the back-and-forth motion of flagella at very short times affects the statistical description of the dynamics. Finally, we show how drag forces modify the characteristics of this particular random walk.

DOI: 10.1103/PhysRevE.83.035301 PACS number(s): 47.63.Gd, 47.50.−d, 47.57.−s, 87.17.Jj

Cell motility [1] is crucial to many biological processes including reproduction, embryogenesis, and infection. Many microorganisms, for example, bacteria, sperm cells, and microalgae, are able to propel themselves. A quantitative understanding of the hydrodynamics of flagella and cilia is thus of great interest [2,3].

One of the peculiarities of the swimming of microorganisms is that it occurs at very low Reynolds numbers, which is very different from our usual experience of swimming at our meter length scale [4,5]. Indeed, when inertia is negligible as compared to viscous forces (i.e., Reynolds number Re is lower than unity), in order to achieve propulsion, swimmers must deform in a way that is not invariant under time reversal. This is known as Purcell's scallop theorem [4]. In living systems, several different strategies are used to achieve propulsion in such conditions: The *E. coli* bacterium uses a rotating flagellum at the "back" of its body, sperm cell propulsion relies on the asymmetry of their flagellar bending waves, the power and recovery strokes of the two front flagella of *Chlamydomonas reinhardtii* (CR) algae are asymmetrical.

Flagellar propulsion in CR induces complex swimming behavior of cells. Over short time scales, the cells undergo an oscillating movement with changes in velocity direction occurring at the same frequency as the beating frequency of flagella. On a time scale longer than the period of beating, average swimming behavior is directional. Eventually, on larger time scales, direction is lost and swimming trajectories resemble a random walk.

CR is a 10-μm motile biflagellated unicellular alga. The cell is spheroidal in shape with two anterior flagella [6]. It belongs to the puller type of swimmers as it uses its front flagella to propel itself, producing a breaststrokelike movement. The swimming direction of the cells can be controlled by stimulus gradients, a phenomenon known as taxis, such as chemotaxis, rheotaxis, or phototaxis. Gradients are not used in our experiments in order to avoid any external tropism on the motility. Wild-type strains were obtained from the Institut de Biologie Physico-Chimique (IBPC) laboratory in Paris [7]. Synchronous cultures of CR were grown in a Tris-acetate phosphate medium using a 12-h/12-h light/dark cycle at 22 °C. Cultures were typically grown for two days under fluorescent lighting before the cells were harvested for experiments.

We studied the swimming dynamics of this microorganism by means of bright field microscopy imaging on an Olympus inverted microscope coupled either to a charge-coupled device (CCD) camera (Sensicam, Photon Lines) used at a frame rate of 10 Hz or to a high-speed CCD camera (Miro, Phantom) used at a frame rate of 400 Hz. Long time experiments used a ×10 magnification lens, whereas we used a ×64 lens for high-speed imaging. Glass chambers (200 μm thick) were coated with bovine serum albumin to prevent cell adhesion. The imaged cells were located 30–60 μm from the glass walls. A red light filter was used in order to prevent phototaxis. Cell tracking [8] was performed using Interactive Data Language with a submicron precision in the detection of hundreds of cells (high-speed experiments) and thousands of cells for long time sequences. To quantify the effect of drag on the cell dynamics, small amounts of short chain dextran (Sigma Aldrich) were added to the culture medium. The chains were short enough for non-Newtonian effects to be absent and long enough to avoid damaging the cells with osmotic effects. This allowed the viscosity η of the medium to be varied between 1.5 and 3.7 mPa s. The range of viscosity is restricted to this interval to ensure the viability of the cells.

Let us first recall the global dynamics of swimming, that is, over time scales of the order of a few seconds. Cell trajectories are found to be correctly modeled by a persistent random walk [9–11]. Cells swim in an almost fixed direction for a typical time of about 1 s. This stage corresponds to a ballistic regime characterized by a mean velocity V. The ballistic regime ends when the swimmers make a turn. A new direction of motion is then observed due to the desynchronization of the pair of flagella [12]. At long time scales, the dispersal properties of the swimmers are randomlike [13,14]. To describe this specific random walk quantitatively, we measured different statistical quantities of interest. Let us first define a persistence angle $\theta(t) = \arccos[\hat{k}(t_0) \cdot \hat{k}(t_0 + t)]$, where $\hat{k}(t)$ is a unitary vector in the direction of movement at time t. Thus, a value of θ close to zero reflects a certain persistence of the trajectory. We measured the probability distribution function of angles θ for different times t. At short time scales, angle distribution peaks at around zero, characterizing the directional persistence in swimming trajectories. Over longer times, we observed a broadening of the distribution and eventually we ended up

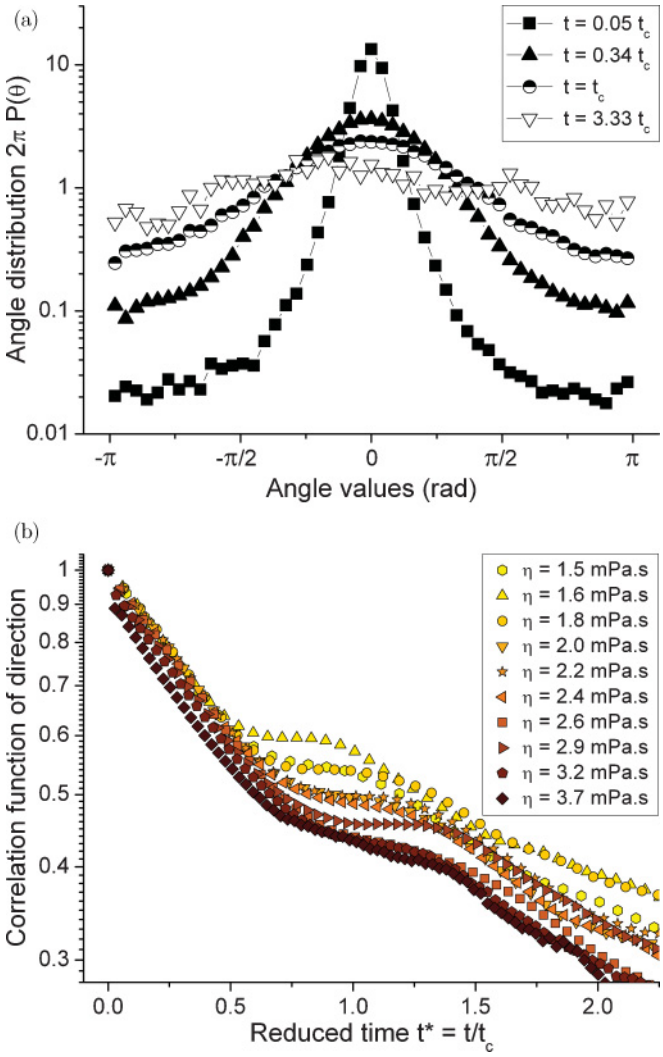

FIG. 1. (Color online) (a) Probability distribution functions of angles $\theta = \arccos[\hat{k}(t_0) \cdot \hat{k}(t_0 + t)]$ for different times t ranging from $0.05t_c$ to $3.33t_c$. Here $t_c = 2.3$ s and the viscosity of the medium is 2.4 mPa s. Only few data points are displayed for the sake of clarity. (b) Correlation functions of direction $C(t/t_c)$ as defined in the text (log-lin scale). Time has been rescaled by the decaying time of an exponential. The different symbols correspond to the viscosities used by varying the concentration of dextran.

with an equidistribution of angle values characteristic of a random walk [Fig. 1(a)]. This phenomenon is even better quantified by looking at the mean value of angle distribution or equivalently at the correlation function of direction defined as $C(t) = \langle \hat{k}(t_0) \cdot \hat{k}(t_0 + t) \rangle$, where $\langle \cdot \rangle$ is an average over time t_0 and over all tracked trajectories. Correlations with infinite decay time [$C(t) = 1$ for all $(t) > 0$] correspond to direction correlations preserved over arbitrarily long times, that is, a purely ballistic regime, whereas a zero lifetime [$C(t) = 0$ for all $(t) > 0$] corresponds to standard random walk behavior [Fig. 1(b)]. The correlation functions decay exponentially over a characteristic time t_c. This correlation time t_c is related to the mean time of persistence over which the direction of swimming is preserved. The different symbols in Fig. 1(b) correspond to experiments where the concentration of short chain dextran was varied, hence modifying the viscosity of the medium from 1.5 to 3.7 mPa s. As viscosity increases, correlation time t_c increases (data not shown) from 1.5 to 3.9 s.

The global dynamics of swimming of CR can thus be described as a correlated random walk characterized by a ballistic regime (with a mean velocity V) and a decorrelation process (over a characteristic time t_c) due to the turns made by the cells. As a consequence, a persistence length $\mathcal{L}$ is naturally defined as the product Vt_c. From a statistical point of view, such a behavior is described by the mean square displacement of cells $\langle r^2(t) \rangle$, which is linear for long times ($t \gg t_c$) and quadratic at shorter times ($t \lesssim t_c$) [13,14]. At even shorter times, the dynamics reflect the consequences of low Reynolds swimming, that is, a nonreciprocal movement of flagella. This then leads to a zigzagging motion of cells due to the back-and-forth motion of flagella [15].

In the present case, cells of diameter $2R \sim 10\ \mu$m are moving at a velocity V around $50\ \mu$m/s in a waterlike medium (viscosity $\eta \sim 1$ mPa s and density $\rho \sim 10^3$ kg/m^3). This represents a very low Reynolds number of the order of $\mathrm{Re} = \rho V R/\eta \sim 2.5 \times 10^{-4}$. The propulsion strategy of CR consists in swimming in a kind of breaststroke where the pair of flagella are wide open during the forward movement and folded along the cell body during the backward movement [16]. Hence, viscous friction is high when the pair of flagella are fully extended during the forward movement and friction is lower during the backward movement. The symmetry under time reversal is thus broken and propulsion is ensured.

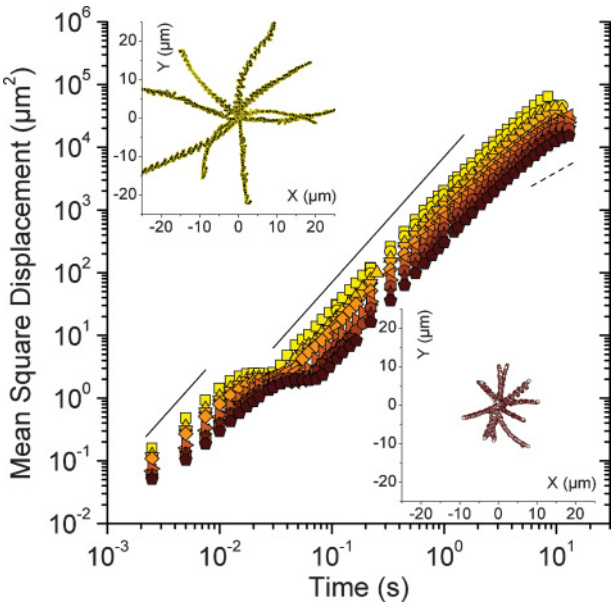

FIG. 2. (Color online) Mean square displacements $\langle r^2(t) \rangle$ of cells as function of time for different viscosities of the medium. The different symbols represent different bath viscosities. The legend for symbols is the same as in Fig. 3(b). The solid lines represent a slope 2 and the dotted line a slope 1 in a log-log scale. Typical two-dimensional (2D) trajectories of a few cells are displayed in the insets. In the top left inset, cells are swimming in the nutritive medium (viscosity $\eta = 1.5$ mPa s), in the lower right corner, the medium is rich in dextran ($\eta = 3.7$ mPa s). Trajectories are represented on the same scale for better comparison and both lasted 0.5 s; their starting positions were all shifted to the origin.

However, because inertia has no role in this regime, this kind of propulsion leads to a back-and-forth movement of the cell in which the velocity is alternatively positive and negative. High-speed imaging (400 Hz) allows us to resolve the very short time dynamics due to flagella beating and thus to study the consequences of this back-and-forth movement on the properties of the swimmers' random walk.

The insets in Fig. 2 show typical cell trajectories imaged at 400 Hz: The back-and-forth movement of swimmers due to the absence of inertia (Re $\ll 1$) together with the long time swimming behavior are visible. In these examples, the cells are swimming either in a nutritive medium of viscosity $\eta = 1.5$ mPa s (top left inset) or in a dextran-rich medium of viscosity 3.7 mPa s (bottom right inset). Cells have a net forward movement corresponding to the power stroke, followed by the recovery stroke that propels the cell backward. As the distance traveled forward is longer than the backward movement, the cells ultimately progress forward. However, these fluctuations in the direction of the velocity have consequences on the measured statistical quantities [17] that we discuss now.

The measured mean square displacement $\langle r^2(t)\rangle$ shows a plateau region at very short time ($t \ll t_c$) that reflects the transition between two quadratic regimes: on the one hand, a fast ballistic regime characterized by the instantaneous velocity u of swimmers and, on the other hand, a slower ballistic regime corresponding to the mean velocity V of swimming which is the resulting forward velocity over several back-and-forth movements. The position of the plateau therefore corresponds to the beating frequency f of the swimmer, which depends on the viscosity of the surrounding medium. To quantify the back-and-forth swimming motion of the cells, we measured

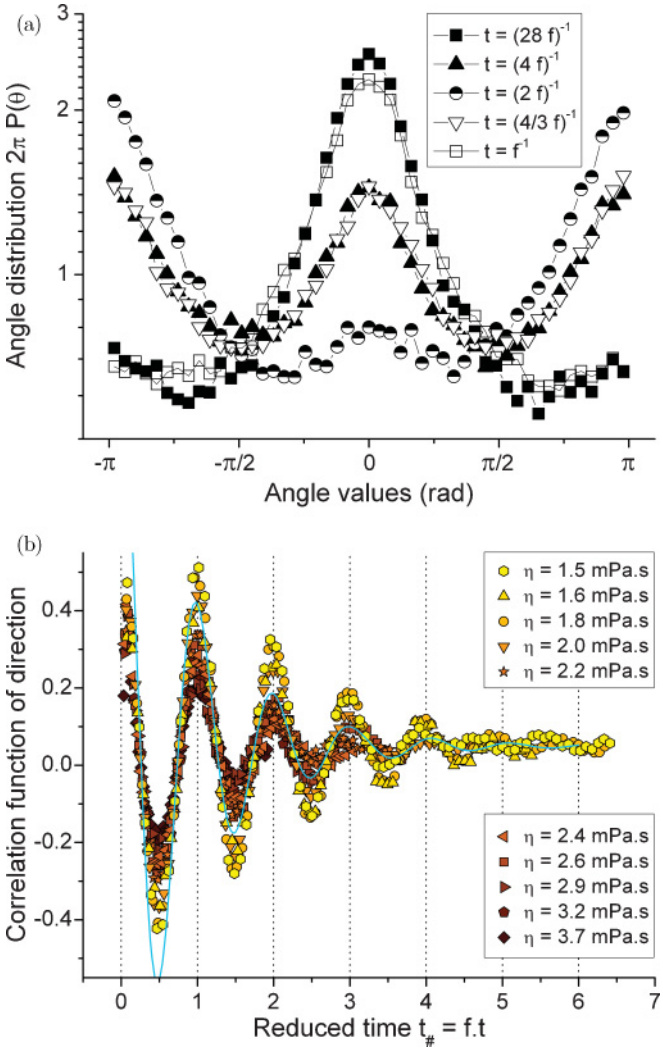

FIG. 3. (Color online) (a) Probability distribution functions of angle θ at short time scales ranging from $t = 1/(28\,f)$ to $t = 1/f$. In these experiments, cells are swimming in a medium of viscosity $\eta = 2.4$ mPa s so that their beating frequency is $f = 14.3$ Hz. (b) Correlation functions of direction as defined in the text. Time has been rescaled with the period $1/f$ of the signal, which corresponds to the beating frequency of flagella. Symbols correspond to different viscosities of the medium. The solid line represents the function $\cos(2\pi t_\#)\exp(-t_\#)$.

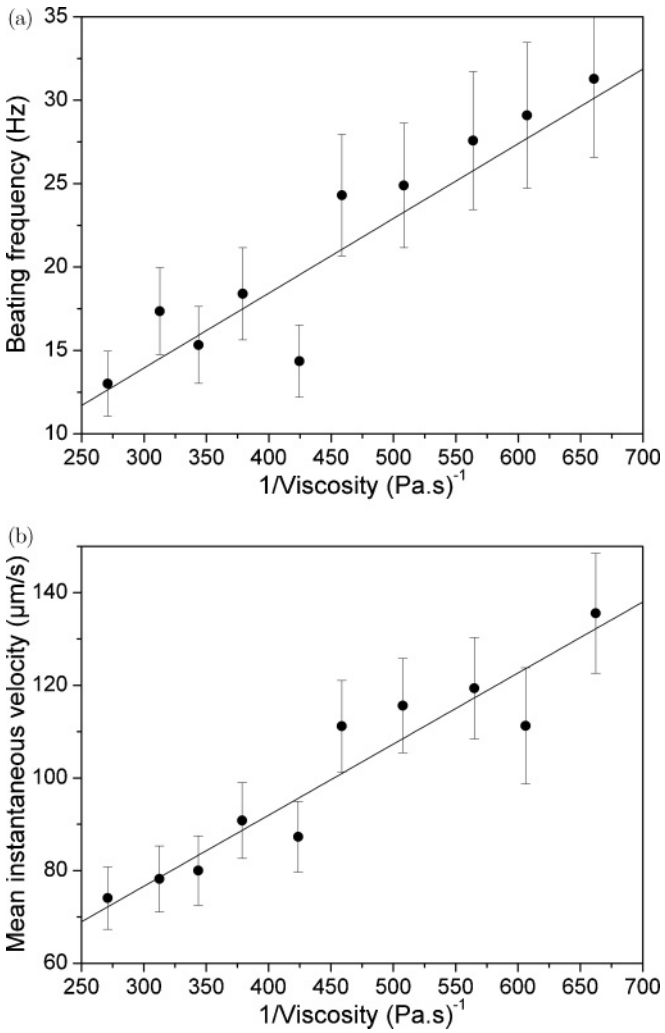

FIG. 4. (a) Beating frequency, obtained from the period of oscillations in the correlation functions of directions, versus the inverse viscosity of the medium. (b) Mean modulus of velocity u as a function of the inverse viscosity of the medium. Solid lines represent linear regression giving: $\eta f = 0.045 \pm 0.01$ Pa and $\eta u = 0.15 \pm 0.04$ Pa μm

the angle probability distribution function. Figure 3(a) shows distribution functions for different times. For a given short time t, the distribution of angles $\theta(t)$ as defined earlier, peaks at around zero, reflecting a given direction at very short time. For longer time scales (close to $1/2f$), anticorrelation in cell direction resulted in new distribution peaks at values of around $\pm\pi$. When a new stroke is produced, the measured angle is again close to zero, giving rise to a peak around zero. Hence, angle distributions have a periodicity which reflects the beating frequency. This is shown in Fig. 3(a) as the distributions are very similar at times shifted by $1/(2f)$, where the typical frequency of the beating f is deduced from the periodical nature of the correlation function of direction. Figure 3(b) shows such correlation functions at varying ft, the product of time multiplied by the fitted frequency of the signal. Data are well described by an exponentially attenuated cosine function. The different symbols correspond to different viscosities of the medium. The exponential decay of the correlation function should reflect the turns in direction the cells eventually perform within a characteristic time t_c. However, due to the 3D nature of the trajectories and the 2D geometry of our setup, correlation was attenuated faster than that.

The other consequence of the fact that swimming is produced at low Reynolds number is that propulsion requires nonzero drag forces. Viscous friction is thus crucial in the dynamics of microswimmers. By varying the viscosity of the medium, we were able to draw some conclusions about the effects of friction forces on the locomotion of microorganisms such as this microalga.

Here, short time dynamics of swimming can be fully described by few mean quantities: flagella frequency beating f [deduced from a cosine fit in Fig. 3(b)] and the mean modulus of instantaneous velocity u, which is the velocity achieved during a power or a recovery stroke. We studied the effects of viscous forces on these quantities. Velocities and beating frequency are found to be inversely proportional to the viscosity of the bath (Fig. 4). As viscosity increases, the beating frequency decreases, varying from 30 to 13 Hz with a viscosity variation from 1.5 to 3.7 mPa s [Fig. 4(a)], giving a slope $\eta f = 0.045 \pm 0.01$ Pa. Accordingly, velocity decreases from 135 to 75 μm/s [Fig. 4(b)] giving a slope $\eta u = 0.15 \pm 0.04$ Pa μm. These results support the idea of imposed-force locomotion [14]. The corresponding stall force, which is proportional to the product $\eta \times u$, is then constant.

The velocity u can be related to the mean propulsion force on the cell body by Stokes' law. Let us now assume that a power stroke (recovery stroke) results from the friction length $\xi_\perp$ ($\xi_\parallel$) of the flagella moving perpendicular (parallel) to its long axis. Moreover, the beating frequency f can be related to the friction of flagella acting on a typical distance of one cell diameter: $6\pi\eta Ru = 2Rf\eta(\xi_\perp + \xi_\parallel)$. Using measurements of the slopes ηu and ηf, we can estimate a sum $\xi_\perp + \xi_\parallel \sim 32$ μm. Using the friction coefficient expressions of a cylinder given in [18], this leads to an aspect ratio of 200 for a 10-μm-long flagellum with a radius of 25 nm. This is a reasonable estimate [6] considering that flagella are not exactly perpendicular and parallel to the flow during power and recovery strokes.

In this work, we quantified the complex dynamics of swimming at short time scale using high-speed microscopy imaging and particle tracking techniques. This study allowed us to analyze the breaststrokelike swimming of a CR cell in a fluid at low Reynolds number and how this swimming is influenced by the viscosity of the ambient fluid. It showed how the friction acting on a CR cell can be qualitatively extracted from the back-and-forth motion of a thin and elongated pair of flagella. This means that a description in terms of time averaged flows is not to be encouraged for such systems [3,19].

This work was financed by the Rhone-Alpes Region (Cible program). We also acknowledge ANR Mosicob for its partial support.

[1] D. Bray, *Cell Movements: From Molecules to Motility* (Routledge, New York, 2001).
[2] S. Ramaswamy, Annu. Rev. Condens. Matter Phys. **1**, 323 (2010).
[3] D. Saintillan, Physics **3**, 84 (2010).
[4] E. M. Purcell, Am. J. Phys. **45**, 3 (1977).
[5] G. Taylor, Proc. R. Soc. Lond. A **209**, 447 (1951).
[6] G. W. D. Stern and E. Harris (editors), in *The Chlamydomonas Sourcebook* (Academic, San Diego, 2008).
[7] *Physiologie Membranaire et Moléculaire du Chloroplaste, Institut de Biologie Physico-Chimique*, Université Pierre et Marie Curie/CNRS UMR 7141, Paris, France.
[8] J. Crocker and D. Grier, J. Colloid Interface Sci. **179**, 298 (1996).
[9] E. Codling, M. Plank, and S. Benhamou, J. R. Soc., Interface **5**, 813 (2008).
[10] C. S. Patlak, Bull. Math. Biophys. **15**, 311 (1953).
[11] J. R. Howse, R. A. L. Jones, A. J. Ryan, T. Gough, R. Vafabakhsh, and R. Golestanian, Phys. Rev. Lett. **99**, 048102 (2007).
[12] M. Polin, I. Tuval, K. Drescher, J. P. Gollub, and R. E. Goldstein, Science **325**, 487 (2009).
[13] K. C. Leptos, J. S. Guasto, J. P. Gollub, A. I. Pesci, and R. E. Goldstein, Phys. Rev. Lett. **103**, 198103 (2009).
[14] S. Rafai, L. Jibuti, and P. Peyla, Phys. Rev. Lett. **104**, 098102 (2010).
[15] W. N. U. Rüffer, Cell Motil. Cytoskeleton **5**, 251 (1985).
[16] D. Ringo, J. Cell Biol. **33**, 543 (1967).
[17] F. Peruani and L. G. Morelli, Phys. Rev. Lett. **99**, 010602 (2007).
[18] M. Tirado, C. Martinez, and J. Delatorre, J. Chem. Phys. **81**, 2047 (1984).
[19] J. S. Guasto, K. A. Johnson, and J. P. Gollub, Phys. Rev. Lett. **105**, 168102 (2010).